Applied Catalysis B: Environmental 88 (2009) 292–298

Contents lists available at ScienceDirect

Applied Catalysis B: Environmental

journal homepage: www.elsevier.com/locate/apcatb

Performance of a catalytically activated ceramic hot gas filter for catalytic tar removal from biomass gasification gas

Manfred Nacken [a,*], Lina Ma [b], Steffen Heidenreich [a], Gino V. Baron [b]

[a] Pall Filtersystems GmbH Werk Schumacher Crailsheim, Zur Flügelau 70, D-74564 Crailsheim, Germany
[b] Department of Chemical Engineering (CHIS), Vrije Universiteit Brussel, Pleinlaan 2, B-1050 Brussels, Belgium

ARTICLE INFO

Article history:
Received 26 August 2008
Received in revised form 2 November 2008
Accepted 9 November 2008
Available online 17 November 2008

Keywords:
Catalytic filter
MgO
NiO
Tar reforming catalyst
Biomass gasification

ABSTRACT

Silicon carbide-based filter elements were catalytically activated to provide filter elements for catalytic tar removal from biomass-derived syngas. The filter element support was coated with CeO_2, $CaO–Al_2O_3$ and MgO with a specific surface of 7.4, 15.9 and 21.9 m^2/g synthesized by exo-templating with activated carbon. Doping of a MgO coated filter element with 60 wt% NiO has led to an increase of the specific surface from 0.15 to 0.21 m^2/g, whereas in case of a $MgO–Al_2O_3$ coated filter element a decrease from 1.18 to 0.91 m^2/g was found. An increase of the NiO loading from 6 to 60 wt% on a MgO coated filter element resulted in an increase of the naphthalene conversion from 91 to 100% at 800 °C and a face velocity of 2.5 cm/s at a naphthalene concentration of 5 g/Nm^3 in model biomass gasification gas. In case of a $MgO–Al_2O_3$ coated filter element with 60 wt% NiO in addition to complete naphthalene conversion in the absence of H_2S, a higher conversion of 66% was found in the presence of 100 ppmv H_2S compared to 49% of the MgO–NiO coated filter element. After scaling up of the catalytic activation procedure to a 1520 mm long filter candle, which shows an acceptable differential pressure of 54.9 mbar, 58 and 97% naphthalene conversion was achieved in the presence and absence of H_2S, respectively. The calculated WHSV value of 209.6 $Nm^3\ h^{-1}\ kg^{-1}$ indicates the technical feasibility of a further increase of the catalytic performance by an increase of the NiO loading.

1. Introduction

More stringent requirements to reduce the global CO_2 emissions and the scarcity of crude oil have stimulated activities to use biomass as a CO_2 neutral feedstock for electricity generation. Gasification techniques allow not only an energy efficient generation of electricity but also the production of synthetic fuels, methane, dimethylether, methanol or hydrogen from the produced syngas by gasifying biomass.

However, in fluidized bed gasifiers using steam, steam and oxygen mixtures or air as gasifying agent, the formation of condensable tar compounds cannot be completely prevented, even if the most advanced dual fluidized bed gasifier technique [1,2] and catalytically active bed material are applied [3,4].

There is a strong need for an efficient, reliable and cost effective tar elimination technique downstream of the gasifier, if the temperature is lowered below 500 °C, to prevent condensation of tars in the subsequent devices e.g. heat exchangers, gas turbine, gas engine or subsequent catalytic conversion units.

Since also dust has to be removed from the syngas, a combination of hot gas filtration with catalytic tar reforming using a catalytic tar reforming filter would be a cost effective way to remove particles and tars from the syngas. In this way, the high temperature of the raw syngas can be exploited for the endothermic tar reforming reaction and no cost intensive reheating is necessary as in case of a two-step gas cleaning consisting of particle separation unit followed by a catalyst unit [5–7]. Furthermore, investment costs are reduced by using only one catalytic filter unit equipped with catalytic hot gas filter elements instead of a two-step cleaning process.

The required reaction temperatures for effective catalytic tar reforming range from 750 to 850 °C [8–14]. At this high temperature silicon carbide is the hot gas filter material of choice due to its high thermal and especially thermoshock resistance.

Catalytic tar reforming hot gas filter elements can be produced by using a special design of a cylindrical catalytic filter element with a porous cylindrical inner tube and filling a tar reforming catalyst into the hollow cylindrical space between the filter element and the inner tube as shown in Fig. 1(a). The catalytic performance of this design up to the prototype scale was already described in detail in previous work [15]. The main advantage of this design is the flexibility to integrate the tailor-made tar

* Corresponding author. Tel.: +49 7951 302 152; fax: +49 7951 26511.
E-mail address: Manfred.Nacken@europe.pall.com (M. Nacken).

0926-3373/$ – see front matter © 2008 Elsevier B.V. All rights reserved.
doi:10.1016/j.apcatb.2008.11.011

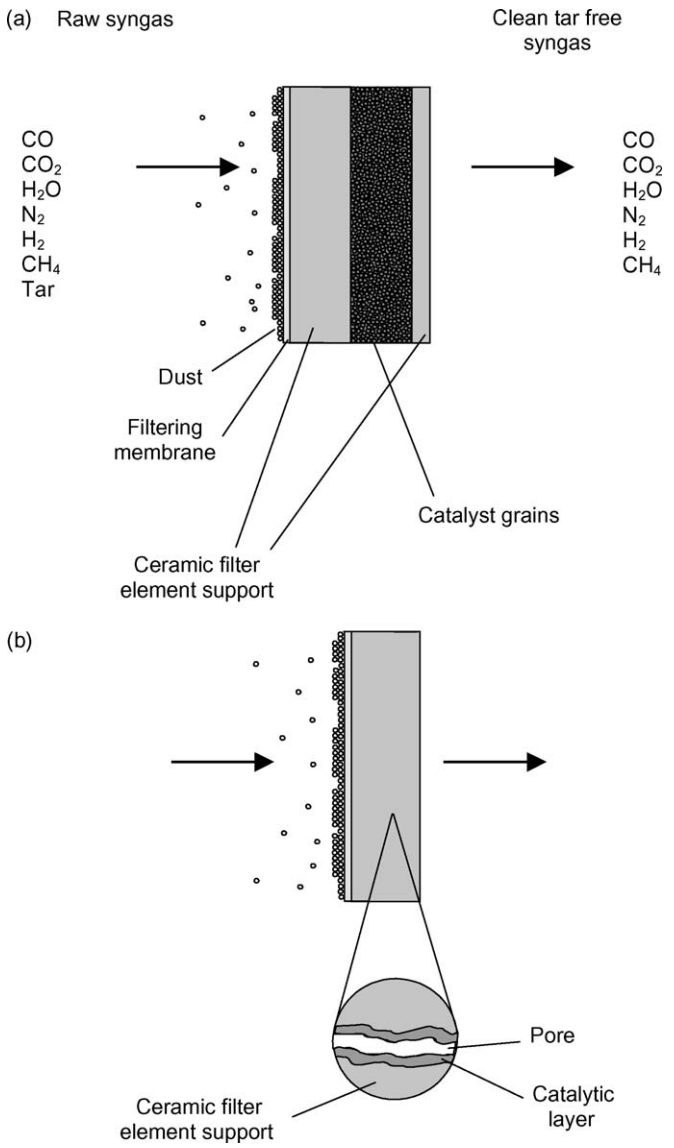

Fig. 1. Schematic design of a tar reforming catalytic filter element with integrated fixed bed (a) or catalytic layer (b).

reforming catalyst for the specific application and the capability to integrate a high amount of catalyst material in this hollow cylindrical space. A disadvantage of this design is the manufacturing of several parts and its assembling in this special filter element design. Furthermore, the face velocity related to the outer surface of the catalytic filter element has to be kept at the lower limit of typical face velocities between 70 and 120 m/h in hot gas filtration in order to keep the face velocity for the integrated catalyst bed at an acceptable value for the catalytic tar reforming reaction. The face velocity related to the outer surface of the fixed bed is a factor of 1.5 higher than the face velocity related to the outer surface of the catalytic filter element caused by the cylindrical design of the catalytic filter element.

With regard to a simplification of the manufacturing process of tar reforming catalytic filter elements and to apply a higher face velocity to reduce the size of the catalytic filter, an alternative integration of the catalyst in the hot gas filter element as catalytic layer by catalytic activation of the 10 mm thick porous silicon carbide filter element would be desirable (Fig. 1(b)).

In previous work such an approach was already successfully applied in the development of a silicon carbide-based catalytic filter element for combined particle separation and NOx removal from laboratory [16] to pilot scale [17]. Furthermore, the feasibilty of the integration of an active tar reforming catalyst as catalytic layer by catalytic activation of 10 mm thick alumina-based filter disks was already shown [18–20].

The main challenge to provide a catalytic tar reforming hot gas filter element by this catalyst integration method is to create a high BET surface area of the catalyst coating on the pore walls of the filter material at high temperatures by depositing the right type and amount of catalyst support material and catalytically active components.

In this work different catalytically activated silicon carbide filter elements prepared by impregnation techniques are examined with respect to their specific surface and catalytic performance in tar removal from biomass gasification gas. The performance of the catalytically most active filter element of this catalytic layer design is then assessed with respect to its technical applicability compared to previous results.

2. Experimental

2.1. Catalyst support material

Basic metal or mixed metal oxide powders were selected as suitable catalyst support materials for the preparation of the catalytic filter elements to prevent poisoning of the Ni catalyst by carbon deposition during the tar reforming reaction. With respect to the requirement of a high BET surface area under the envisaged operating temperature of 800 °C of the catalytic filter element, MgO, $CaO–Al_2O_3$ and CeO_2 powders were manufactured according to the exo-templating procedure of Schwickardi et al. [21]. Activated carbon with a BET surface of 793 m^2/g was used and impregnated with the appropriate aqueous metal nitrate solutions given in Table 1, followed by drying at 35 °C. After calcination of the dried metal nitrate impregnated activated carbon powders at 800 °C the MgO, $CaO–Al_2O_3$ and CeO_2 powders were obtained as fine particulate powder with the BET surfaces given in Table 1.

In addition, appropriate commercially available carbonate-based precursors were used to prepare a fine particulate MgO–CaO (50:50 wt%) and a $MgO–Al_3O_3$ (70:30 wt%) powder after 5 h calcination at 900 °C, denoted as MgCa and MgAl, respectively. The corresponding BET surfaces after calcination at 900 °C are 15.6 m^2/g and 41.3 m^2/g, respectively.

Table 1
Preparation parameters for MgO, $CaO–Al_2O_3$ and CeO_2 oxide powders by exo-templating with activated carbon and corresponding BET surfaces.

Oxide powder	Notation	Precursor	Precursor concentration (mol/l)	Mass ratio precursor/ activated carbon	BET surface after 24 h calcination at 800 °C (m^2/g)
MgO	Mg	$Mg(NO_3)_2 \times 6H_2O$	1.56	0.414	21.9
$CaO–Al_2O_3$	CaAl	$Ca(NO_3)_2 \times 4H_2O$ $Al(NO_3)_3 \times 9H_2O$	0.45 1.14	0.159 0.640	15.9
CeO_2	Ce	$Ce(NO_3)_3 \times 6H_2O$	0.52	0.234	7.4

2.2. Preparation of catalyst support coated filter elements

A silicon carbide (SiC)-based hot gas filter element of the type "DIA-SCHUMALITH®" with a fine filtering mullite outer-membrane and the dimension 60/40 mm (outer diameter/inner diameter) × 50 mm (length) was used as filter body for the catalyst support coating. For the laboratory scale preparation 50 mm long filter cylinders and for pilot scale 1520 mm long cylindrical filter elements were used.

The appropriate catalyst support coated SiC filter elements were prepared by using the corresponding fine-wet milled suspensions of the three above-mentioned oxide powders and the two carbonate-based precursors for impregnation according to the incipient wetness technique. The solid content related to the final metal or mixed metal oxide was adjusted to 7 wt% in all prepared catalyst support material suspensions except of the MgO–CaO and MgO–Al_2O_3 precursor suspensions, where a solid content of 6% was adjusted.

The impregnated filter cylinders were dried at 25 °C in an air stream under horizontal rotation followed by sintering at 900 °C to obtain the catalyst support coated filter elements denoted e.g. as SiC–MgAl and SiC–MgAl (T) in the following, if e.g. MgO–Al_2O_3 was used as catalyst support material on laboratory scale or pilot scale, respectively.

2.3. Catalytic activation of catalyst support coated filter elements

Catalyst support coated filter cylinders to be used in a subsequent catalytic activation were prepared without the final sintering step. Only in case of sample SiC–MgAl a thermal treatment for dehydration of the coated filter cylinder was applied after drying. The as-prepared catalyst support coated filter cylinders were catalytically activated by impregnation with the appropriate aqueous solution of nickel nitrate hexahydrate ($Ni(NO_3)_2 \times 6H_2O$) followed by drying at 25 °C in an air stream and sintering at 900 °C to adjust NiO loading amounts of 6 and 60 wt% related to the loading amount of the catalyst support material. The obtained catalytically activated filter elements were denoted e.g. SiC–MgAl–60Ni or SiC–MgAl–60Ni (T) depending on laboratory or pilot scale preparation, respectively.

2.4. Characterization

2.4.1. Particle size distribution

The particle size distribution of the precursor suspensions MgCa and MgAl were measured using acoustic spectroscopy with a spectrometer (DT-1200, Quantachrome). Ultrasound pulses were directed through the undiluted suspensions and the attenuation of the pulses were detected in a wide frequency range between 1 and 100 MHz to calculate the corresponding particle size distributions and the average particle sizes as median (D50) values.

2.4.2. BET surface

The BET (specific) surface of catalyst support coated and catalytically activated filter cylinders were determined on monolithic pieces of the dimension 8 mm × 10 mm with krypton as test gas on a Quantachrome Autosorb-3 with a measurement error of 0.005 m^2/g.

Powder samples were measured with N_2 as test gas with a measurement error of 0.03 m^2/g. Before the measurements the samples were dried at 200 °C for 5 h under vacuum.

2.4.3. Differential pressure

The differential pressure of the upscaled and catalytically activated filter cylinder was examined by adjusting different face velocities related to the outer surface of the filter cylinder. The cylinder was vertically fixed in an appropriate differential pressure test rig by sealing the front and end part of the filter cylinder and passing the corresponding volume flow to the selected face velocity from the inner to the outer surface of the porous filter cylinder. The resulting flow resistance was measured as differential pressure with a measurement error of ±0.2 mbar.

2.4.4. Measurement of the catalytic activity

The catalytic activity of catalytic filter samples in tar removal from biomass gasification gas was measured under comparable conditions as described in detail in previous work [15]. An electrically heated tube reactor, a mass spectrometer and a model biomass gasification gas of the composition of 50% N_2, 12% CO, 10% H_2, 11% CO_2, 5% CH_4 and 12% H_2O with a concentration of the tar model compound naphthalene of 5 g/N m^3 was used. For the catalyst deactivation studies, a H_2S containing model biomass gasification gas with a H_2S content of 100 ppmv was used.

The naphthalene conversion measurements were performed at distinct temperature points within the temperature range between 700 and 900 °C by adjusting at all temperature points a constant face velocity of 90 m/h related to the outer surface of a disk sample of 28 mm outer diameter. This corresponds to a gas hourly space velocity (GHSV) of 2080 h^{-1}. No pretreatment of the catalytic filter samples was performed. For activation, the NiO containing catalytic filter samples were reduced in situ during the increase of the temperature up to 700 °C.

For the determination of the catalytic activity of laboratory scale filter samples catalytically activated silicon carbide filter disks of the dimension 28 mm (outer diameter) × 10 mm (thickness) were prepared by applying the same preparation procedure as developed for catalytically activated filter cylinders. This was necessary to reduce the dimension of the required measurement test rig, the gas consumption and to simplify the catalyst screening.

Catalytically activated disks denoted e.g. SiC–Mg–60Ni (D) were fixed in an Al_2O_3 reactor tube of the dimension 36/29 mm × 500 mm using an Al_2O_3 cement material without affecting the filtration surface of the disk.

For the examination of the catalytic activity of the upscaled most catalytically active filter element of the dimension 60/40 mm × 1520 mm, a circular segment of the dimension 28 mm × 10 mm was drilled out and mounted in an Al_2O_3 reactor tube. In a first approximation this sample can be used like a filter disk in spite of a slight curvature.

3. Results and discussion

3.1. Catalyst support coated filter elements

Silicon carbide hot gas filter elements of the type "DIA-SCHUMALITH®" are manufactured by high temperature grain sintering leading to a relatively low BET surface area of 0.013 m^2/g for the uncoated hot gas filter element.

With respect to the preparation of catalytically activated SiC hot gas filter elements with high catalytic performance in tar reforming, the SiC filter body has to be surface modified with a suitable catalyst support material to provide a sufficiently high specific surface for a high dispersion of the catalytically active component. Based on results of the previous work [15], basic support materials such as MgO and CaO–Al_2O_3 have proven to be excellent supports for catalytic tar reforming.

Therefore, several impregnation suspensions using MgO, CaO–Al_2O_3 mixed oxide and CeO_2 synthesized by exo-templating were prepared. In addition, two carbonate-based precursor suspensions of a MgO–CaO and a MgO–Al_2O_3 mixed oxide were used to examine the effect of using a catalyst support material with high internal porosity.

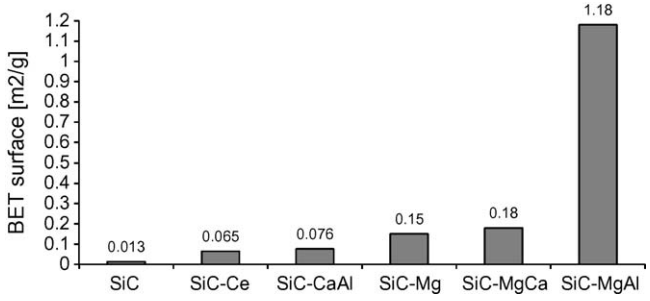

Fig. 2. BET surface of different catalyst support coated SiC filter cylinders and of the uncoated filter cylinder.

The corresponding BET surface of the five catalyst support coated filter cylinders are presented in Fig. 2.

Fig. 2 shows that the BET surface of the SiC filter element can be increased by a factor of 5 (sample SiC–Ce) up to a factor of 91 (SiC–MgAl) by selecting the right catalyst support material.

The coating of SiC cylinders with the synthesized oxide powders CeO_2, $CaO–Al_2O_3$ and MgO exhibiting BET surfaces of 7.4, 15.9 and 21.9 m^2/g (see Table 1) leads to appropriate BET surfaces in a similar increasing order from 0.065 over 0.076 up to 0.15 m^2/g. In the comparison of sample SiC–Ce and SiC–Mg it is shown, that an increase of the BET surface of a catalyst support coated filter element by a factor of 2.3 is possible, if the BET surface of the starting metal oxide powder is increased by a factor of 2.8.

Sample SiC–MgCa with a BET surface of 0.18 m^2/g confirms this trend of creating a higher BET surface of the catalyst support coated filter element, if one starts from a higher BET surface of the oxide powder that was 15.6 m^2/g at 900 °C for this sample.

Surprisingly, sample SiC–MgAl prepared with $MgO–Al_2O_3$ exhibiting in powder form a BET surface of 41.3 m^2/g at 900 °C due to pore formation by carbonate decomposition and dehydration shows a higher BET surface (1.18 m^2/g) than the expected BET surface of about 0.5 m^2/g compared to SiC–MgCa. For this reason the corresponding particle size distribution of both impregnation suspensions was analyzed in more detail.

Additionally, the BET surfaces of the fine-wet milled MgO–CaO and $MgO–Al_2O_3$ powders of the corresponding impregnation suspensions were measured after evaporation of the solvent and sintering at 900 °C under the same conditions as the catalyst support coated filter cylinders SiC–MgCa and SiC–MgAl. The obtained BET surface values of these fine-wet milled bulk materials are presented in Fig. 3. For comparison, the calculated BET surface contributions only related to the catalyst support material MgO–CaO or $MgO–Al_2O_3$, respectively, in the catalyst support coated filter cylinders SiC–MgCa and SiC–MgAl with a monolitic BET surface of 0.18 and 1.18 m^2/g are also presented.

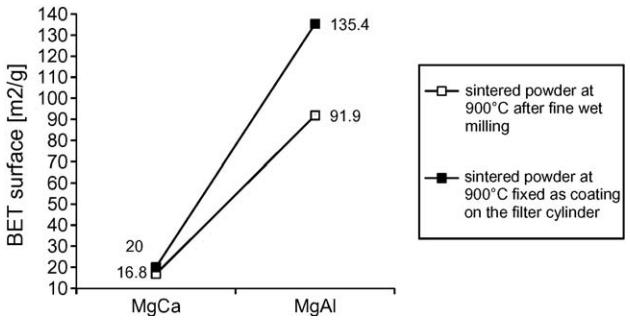

Fig. 3. BET surface of the fine-wet milled catalyst support powders MgO–CaO and $MgO–Al_2O_3$ in form of the bulk material and as coating material on the filter cylinder.

Fig. 3 shows that the BET surface of the $MgO–Al_2O_3$ bulk powder is with 91.9 m^2/g by a factor of 5.5 higher than the one of the MgO–CaO bulk powder (16.8 m^2/g). This result indicates that the higher BET surface of the filter cylinder SiC–MgAl (Fig. 2: 1.18 m^2/g) compared to SiC–MgCa (0.18 m^2/g) is due to the difference in internal porosity, considering the relatively large average particle size of 208 nm for $MgO–Al_2O_3$ and 80 nm for MgO–CaO.

Furthermore, it is shown that the specific surfaces of the $MgO–Al_2O_3$ and MgO–CaO bulk materials are distinctly lower than the appropriate BET surfaces of the mixed oxides as coating material on the filter cylinders. This is probably due to the separation of the oxide particles from each other on the pore wall surface of the filter cylinders and thereby preventing their sintering together. This behaviour is especially pronounced in case of the catalyst support material $MgO–Al_2O_3$. This can be explained by the larger average particle size of $MgO–Al_2O_3$ in comparison to MgO–CaO, exhibiting a lower driving force in sintering of the particles together than in case of MgO–CaO.

3.2. Catalytically activated filter elements

In previous work it was found that a fixed bed catalyst based on MgO grains with a BET surface area of 0.15 m^2/g is sufficient to provide a highly active tar reforming catalyst after catalytic activation with NiO [15]. Thus, NiO doping of the MgO coated filter cylinder SiC–Mg providing the same BET surface (Fig. 2: 0.15 m^2/g) seemed to be promising. Two catalytic filter cylinders with a NiO loading of 6 and 60 wt% were prepared to study the effect of the NiO loading on the BET surface (Fig. 4). Additionally, for examination of the support effect on the specific surface at a high NiO loading a $MgO–Al_2O_3$ coated catalytic filter cylinder providing a BET surface of 1.18 m^2/g was doped with 60 wt% NiO.

A 6 and 60 wt% NiO doping increases the specific surface of a MgO coated filter element by 73 and 40% to 0.26 and 0.21 m^2/g, respectively, whereas a 60% NiO doping slightly reduces the specific surface of a $MgO–Al_2O_3$ coated filter element by 23% to 0.91 m^2/g (Fig. 4). This contrary effect of NiO doping is due to the large difference in the internal porosity. In the MgO coated filter element with low internal porosity NiO is mainly deposited on the MgO support and creates additional surface by NiO crystallite formation. In case of the $MgO–Al_2O_3$ coated filter cylinder NiO doping leads to a partial pore filling of the highly porous $MgO–Al_2O_3$ coating and a smoothing of the surface. Nevertheless, this sample provides the largest catalytic surface of these series and, therefore, seemed to be predestined for a high catalytic activity.

3.3. Catalytic performance in tar reforming

The three catalytic layer systems Mg–6Ni, Mg–60Ni and MgAl–60Ni in Fig. 4 deposited in a SiC filter disk were examined on their catalytic activity in naphthalene reforming as function of the reaction temperature with a model biomass gasification gas. The

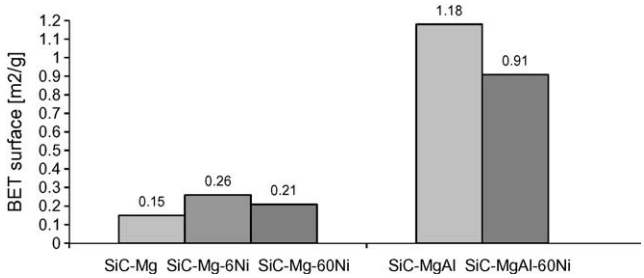

Fig. 4. BET surface of the catalyst support coated filter cylinders SiC–Mg and SiC–MgAl before and after doping with 6 or 60 wt% NiO, respectively.

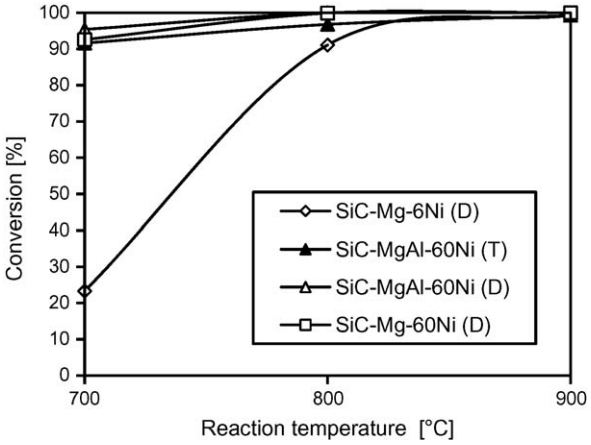

Fig. 5. Naphthalene conversion of different catalytically activated filter disks and one filter segment of the upscaled catalytic filter candle as a function of the reaction temperature at a face velocity of 90 m/h in the absence of H_2S.

naphthalene conversion results in the absence and presence of a typical concentration of 100 ppmv H_2S are presented in Figs. 5 and 6, respectively. Additionally, the corresponding conversion results of a circular segment of the catalytically activated SiC cylinder after scale up to a 1520 mm long catalytic filter candle of commercial size (sample SiC–MgAl–60Ni (T)) are presented in the absence (Fig. 5) and presence of H_2S (Fig. 6).

In the absence of H_2S and at 900 °C the three catalytically activated filter samples SiC–Mg–6Ni (D), SiC–Mg–60Ni (D) and SiC–MgAl–60Ni (D) show complete conversion of naphthalene independently of their NiO loading and specific surface (Fig. 5).

At the envisaged hot gas filtration temperature of 800 °C for combined particle separation and catalytic tar removal only the filter samples SiC–Mg–60Ni and SiC–MgAl–60Ni with a NiO loading amount of 60 wt% NiO show complete naphthalene conversion, whereas the sample SiC–Mg–6Ni with 6 wt% NiO converts naphthalene only to an extent of 91%. Evidently, the NiO loading has a strong influence on the catalytic tar removal. This result is even more pronounced at 700 °C leading to naphthalene conversions of 95, 93 and 23% for the samples SiC–MgAl–60Ni (D), SiC–Mg–60Ni (D) and SiC–Mg–6Ni (D) indicating their sequence of decreasing catalytic activity.

The corresponding naphthalene conversions at 900, 800 and 700 °C of the most active catalytic filter sample after scale up to a catalytic filter candle of commercial size (sample SiC–MgAl–60Ni (T)) are with 99, 97 and 92% only by 1, 3 or 8% lower than the corresponding conversion values measured on the corresponding catalytically activated disk SiC–MgAl–60Ni (D). The small differences in the conversion values are probably due to differences in catalyst distribution resulting from the differences in the drying procedure of the disk and the 1500 mm long filter candle in an air stream. Apart from these small differences, the naphthalene conversion results show, that the developed procedure for catalytic activation of SiC filter cylinders is scalable. Thus, catalytic filter candle prototypes with a tar removal performance of 97% at 800 °C and 99% at 900 °C can be produced. Furthermore, the method developed for direct determination of the catalytic activity by cutting a circular segment out of the catalytic filter candle has proven to be suitable.

In the presence of 100 ppmv H_2S, that is formed during gasification of sulfur containing compounds in the biomass, strong deactivation of the catalytically activated filter disks SiC–Mg–6Ni (D), SiC–Mg–60Ni (D) and SiC–MgAl–60Ni (D) is found and this deactivation increases when decreasing the temperature from 900 to 700 °C (Fig. 6).

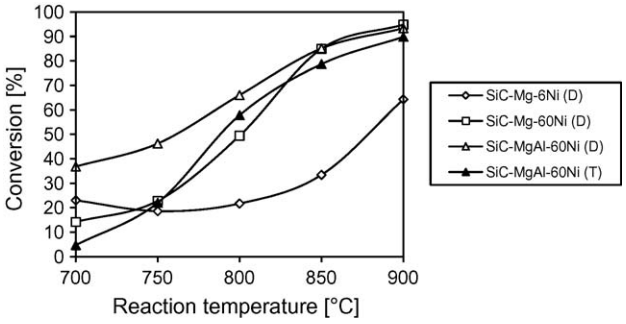

Fig. 6. Naphthalene conversion of different catalytically activated filter disks and one filter segment of the upscaled catalytic filter candle as a function of the reaction temperature at a face velocity of 90 m/h in the presence of 100 ppmv H_2S.

Stronger adsorption of H_2S at lower temperature leads to increased H_2S blocking of Ni active sites and may result in deactivation by carbon deposition. Carbon deposition as further reason of Ni catalyst deactivation is a consequence of incomplete reforming by a decreased catalytic conversion rate.

At 900 °C the catalytic filter samples with a high NiO loading SiC–Mg–60Ni (D) and SiC–MgAl–60Ni (D) show a naphthalene conversion of 93 and 95%, whereas the sample with the tenfold lower NiO content shows only a conversion of 64%. This indicates that blocking of a part of Ni active sites by H_2S molecules leads to a stronger deactivation, if a smaller amount of Ni active sites is provided.

At 800 °C the catalytic filter sample SiC–MgAl–60Ni shows with 66% naphthalene conversion the highest catalytic activity and a distinctly higher conversion than sample SiC–Mg–60Ni (49%). This can be attributed to the difference in the specific surface of the catalyst support material. In case of sample SiC–MgAl–60Ni (D) a better dispersion of the active component is possible leading to more and smaller Ni crystallites, where a larger fraction of the Ni sites remained unblocked by H_2S.

The corresponding naphthalene conversion at 800 °C of the most catalytically active filter sample after scale up to the commercial scale dimension SiC–MgAl–60Ni (T) still shows a conversion of 58%. This value is by 8% lower than the conversion value measured on the corresponding catalytically activated filter disk (SiC–MgAl–60Ni (D)) indicating a similar small conversion difference as found in the absence of H_2S due to the above-mentioned reason (Fig. 5).

For the assessment of the catalytic performance of the developed catalytically activated filter element SiC–MgAl–60Ni (T) with regard to its technical applicability under H_2S containing biomass gasification gas conditions, the naphthalene conversion at 800 °C in the presence of H_2S is correlated with the corresponding

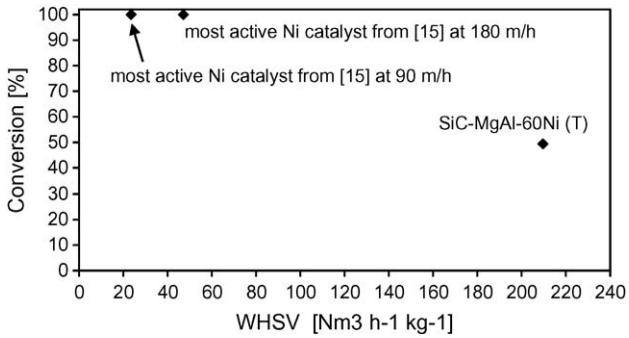

Fig. 7. Correlation between the appropriate naphthalene conversions at 800 °C in the presence of 100 ppmv H_2S of the most active Ni catalyst from [15] at a face velocity of 90 and 180 m/h and of the sample SiC–MgAl–60Ni (T) at a face velocity of 90 m/h with the corresponding WHSV values.

weight hourly space velocity (WHSV) related to the loading amount of NiO in Fig. 7. For comparison, the corresponding naphthalene conversion values at a face velocity of 90 and 180 m/h of the developed most active Ni catalyst for a catalytic filter element with a fixed bed design (Fig. 1(a)) [15] are correlated with the corresponding WHSV values.

Fig. 7 shows that a decrease of the WHSV value from 209.6 (sample SiC–MgAl–60Ni (T)) to 23.6 $Nm^3\ h^{-1}\ kg^{-1}$ (Ni catalyst at 90 m/h) leads to an increase of the naphthalene conversion from 58 to 100% [15] in the presence of H_2S at the same face velocity of 90 m/h. Complete naphthalene conversion was also found by operating the Ni catalyst at a double face velocity that corresponds to a WHSV value of 47.2 $Nm^3\ h^{-1}\ kg^{-1}$. Thus, complete naphthalene conversion is theoretically feasible with a catalytically activated filter element, if one e.g. increase the NiO loading by a factor of 4.4 by applying a face velocity of 90 m/h. If a lower face velocity of e.g. 72 m/h is selected, that is still in the range of face velocities typical for hot gas filtration, an increase of the NiO loading by a factor of 3.6 would be necessary to achieve complete naphthalene conversion with a catalytically activated filter element. An increase of the NiO loading to the extent of the calculated factor should at least be approached, if it is intended to select a compromise between the increase of the NiO loading and the differential pressure of the catalytically activated filter element. A higher NiO loading can be realized by increasing the BET surface of the catalyst support, which is the objective of further preparation work to allow a sufficient dispersion of the necessary higher NiO amount.

In this way a catalytically activated filter element would be accessible that is highly active in tar reforming also in the presence of 100 ppmv H_2S.

In the absence of H_2S, that can be realized by effective H_2S removal by means of sorbent injection, the developed catalytically activated filter element SiC–MgAl–60Ni (T) shows already 97% naphthalene conversion at 800 °C and a face velocity of 90 m/h (Fig. 5).

3.4. Differential pressure

The differential pressure of a catalytically activated tar reforming filter element is an important characteristic and was examined for the upscaled catalytic filter element SiC–MgAl–60Ni (T), before and after catalytic activation as a function of the face velocity (Fig. 8).

After extrapolation of the differential pressure curves of the uncoated and upscaled catalytically activated filter element SiC–MgAl–60Ni (T) to the face velocity of 90 m/h that corresponds to 2.5 cm/s, the differential pressure of the uncoated SiC hot gas filter element is 8 mbar and the one of the catalytically activated filter element is 22.7 mbar at 25 °C. The differential pressure increase of 14.7 mbar by the catalytic activation can be explained by a slight pore size reduction of the porous SiC filter structure by the pore wall catalyst coating and an increase of the surface roughness. Thus, the differential pressure of the catalytically activated tar reforming filter element under operating conditions (800 °C) is with 54.9 mbar only slightly higher than the differential pressure of the developed tar reforming catalytic filter element with a fixed bed design of previous work (Fig. 1(a)) showing a differential pressure value of 47.9 mbar at 800 °C [15].

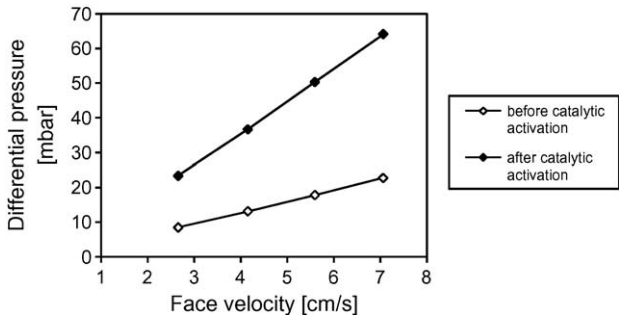

Fig. 8. Differential pressure of the catalytically activated filter element SiC–MgAl–60Ni (T) as a function of the face velocity at 25 °C by using air.

It can be summarized, that catalytic activation of a porous SiC filter body has proven to be an alternative and more simple manufacturing method to provide tar reforming catalytic filter element prototypes with acceptable differential pressures that are to be tested on pilot scale under real biomass gasification gas conditions after further optimization of the catalytic performance.

4. Conclusions

Catalytically active SiC hot gas filter elements for catalytic tar removal from biomass gasification gas with a sufficiently high monolithic BET surface of >0.2 m^2/g were prepared by impregnation and catalytic activation using a catalyst support starting powder of a high BET surface of at least >20 m^2/g, that can be tailor-made by applying the exo-templating procedure followed by doping with a sufficiently high loading amount of 60 wt% NiO. In case of a SiC filter element catalytically activated with a MgO–NiO catalyst coating, a complete conversion of the tar model compound naphthalene was achieved at 800 °C in the absence of H_2S applying a face velocity of 90 m/h. Using MgO–Al_2O_3–NiO as catalytic coating that exhibits a higher monolithic BET surface of 0.91 m^2/g due to a higher internal porosity of the catalyst support material an increase of the naphthalene conversion from 49 to 66% was achieved in the presence of 100 ppmv H_2S. After scale up of the corresponding catalytic activation procedure to a catalytic filter element of 1520 mm length comparable naphthalene conversions of 97% in the absence and 58% in the presence of H_2S were found. The 54.9 mbar differential pressure under operating conditions is acceptable. Comparing the WHSV value of a MgO–Al_2O_3–NiO activated SiC filter element with that of the developed fixed bed catalyst of previous work [15] indicates that a further optimization of the catalytic performance is technically feasible to provide a comparably active tar reforming catalytic filter element prototype for pilot testing under real H_2S containing biomass gasification gas.

References

[1] C. Pfeifer, R. Rauch, H. Hofbauer, Ind. Eng. Chem. Res. 43 (2004) 1634–1640.
[2] J. Corella, J.-M. Toledo, G. Molina, Int. J. Oil Gas Coal Technol. 1 (1/2) (2008) 194–207.
[3] L. Devi, K.J. Ptasinski, F.J.J.G. Janssen, Fuel Process. Technol. 86 (2005) 707–730.
[4] C. Pfeifer, R. Rauch, H. Hofbauer, D. Świerczyński, C. Courson, A. Kiennemann, in: A.V. Bridgwater, D.G.B. Boocock (Eds.), Science in Thermal and Chemical Biomass Conversion, vol. 1, CPL Press, 2006, pp. 677–690.
[5] J. Corella, J.-M. Toledo, R. Padilla, Ind. Eng. Chem. Res. 43 (2004) 2433–2445.
[6] J.M. Toledo, J. Corella, G. Molina, Ind. Eng. Chem. Res. 45 (2006) 1389–1396.
[7] R. Zhang, R.C. Brown, A. Suby, K. Cummer, Energy Convers. Manage. 45 (2004) 995–1014.
[8] M.P. Aznar, M.A. Caballero, J. Gil, J.A. Martin, J. Corella, Ind. Eng. Chem. Res. 37 (1998) 2668–2680.
[9] D. Sutton, B. Kelleher, J.R.H. Ross, Fuel Process. Technol. 73 (2001) 155–173.
[10] W. Torres, S.S. Pansare, J.G. Goodwin, Catal. Rev. 49 (2007) 407–456.
[11] E.G. Baker, L.K. Mudge, M.D. Brown, Ind. Eng. Chem. Res. 26 (1987) 1335–1339.
[12] C.M. Kinoshita, Y. Wang, J. Zhang, Ind. Eng. Chem. Res. 34 (1995) 2949–2954.
[13] D.N. Bangala, N. Abatzoglou, J.-P. Martin, E. Chornet, Ind. Eng. Chem. Res. 36 (1997) 4184–4192.
[14] D. Świerczyński, S. Libs, C. Courson, A. Kiennemann, Appl. Catal. B: Environ. 74 (2007) 211–222.

[15] M. Nacken, L. Ma, K. Engelen, S. Heidenreich, G.V. Baron, Ind. Eng. Chem. Res. 46 (2007) 1945–1951.
[16] M. Nacken, S. Heidenreich, M. Hackel, G. Schaub, Appl. Catal. B: Environ. 70 (2007) 370–376.
[17] S. Heidenreich, M. Nacken, M. Hackel, G. Schaub, Powder Technol. 180 (2008) 86–90.
[18] K. Engelen, Y. Zhang, D.J. Draelants, G.V. Baron, Chem. Eng. Sci. 58 (2003) 665–670.
[19] L. Ma, H. Verelst, G.V. Baron, Catal. Today 105 (2005) 729–734.
[20] L. Ma, G.V. Baron, Powder Technol. 180 (2008) 21–29.
[21] M. Schwickardi, T. Johann, W. Schmidt, F. Schüth, Chem. Mater. 14 (2002) 3913–3919.